Host-Specific and Homologous Pairs of *Melampsora larici-populina* Effectors Unveil Novel *Nicotiana benthamiana* Stromule Induction Factors

Claire Letanneur,[1] Alexandre Brisson,[1] Mathias Bisaillon,[1] Théo Devèze,[1] Mélodie B. Plourde,[1] Martin Schattat,[2] Sébastien Duplessis,[3] and Hugo Germain[1],[†] 🄳

[1] Chemistry, Biochemistry, and Physics Department, Université du Québec à Trois-Rivières, Trois-Rivières, G8Z 4M3, Canada
[2] Plant Physiology Department, Martin Luther University, 06120 Halle, Germany
[3] Université de Lorraine, INRAE, IAM, F-54000 Nancy, France

The poplar rust fungus *Melampsora larici-populina* is part of one of the most devastating group of fungi (Pucciniales) and causes important economic losses to the poplar industry. Because *M. larici-populina* is a heteroecious obligate biotroph, its spread depends on its ability to carry out its reproductive cycle through larch and then poplar parasitism. Genomic approaches have identified more than 1,000 candidate secreted effector proteins (CSEPs) from the predicted secretome of *M. larici-populina* that are potentially implicated in the infection process. In this study, we selected CSEP pairs (and one triplet) among CSEP gene families that share high sequence homology but display specific gene expression profiles among the two distinct hosts. We determined their subcellular localization by confocal microscopy through expression in the heterologous plant system *Nicotiana benthamiana*. Five out of nine showed partial or complete chloroplastic localization. We also screened for potential protein interactors from larch and poplar by yeast two-hybrid assays. One pair of CSEPs and the triplet shared common interactors, whereas the members of the two other pairs did not have common targets from either host. Finally, stromule induction quantification revealed that two pairs and the triplet of CSEPs induced stromules when transiently expressed in *N. benthamiana*. The use of *N. benthamiana eds1* and *nrg1* knockout lines showed that CSEPs can induce stromules through an *eds1*-independent mechanism. However, CSEP homologs shared the same impact on stromule induction and contributed to discovering a new stromule induction cascade that can be partially and/or fully independent of *eds1*.

Keywords: chloroplast, EDS1, effector, host specificity, NRG1, Pucciniales, rust fungi, stromules

[†]Corresponding author: H. Germain; hugo.germain@uqtr.ca

Pucciniales, the order of the rust fungi, threatens worldwide security, as rust fungi infect most of the crops cultivated for food and bioresources (van Esse et al. 2020). Moreover, economic exchanges, environmental changes, and global warming will increase the spread of these pathogens (Brasier 2008; Chaloner et al. 2021). Despite being an important threat, rust fungi are still understudied because of technical barriers such as their difficult cultivation on synthetic media or the lack of post-genomic and post-transcriptomic research tools (Petre and Duplessis 2022). *Melampsora larici-populina* is a heteroecious obligate biotroph that must parasitize larch and poplar to complete its life cycle (Hacquard et al. 2011). Its spread causes extensive production loss in poplar cultures. This tripartite pathosystem is a promising model of study, thanks to the availability of genomic and transcriptomic resources (Duplessis et al. 2011, 2021; Kuzmin et al. 2019; Lorrain et al. 2019; Sun et al. 2022; Tuskan et al. 2006). In the past, *M. larici-populina* showed a high capability of resistance breakdown in poplar plantations, making production of resistant monoclonal poplar inefficient (Persoons et al. 2017; Pinon and Frey 2005). Such an ability to overcome complete resistance may reflect a high diversity of candidate secreted effector proteins (CSEPs) driven by high and complex selective pressure caused by its obligate biotrophy. In general, CSEPs are small proteins that share common characteristics such as a relatively short size, a signal peptide, and a rather high number of cysteines. A total of 1,184 CSEPs have been reported in *M. larici-populina* (Hacquard et al. 2010, 2012). CSEPs' functional characterization can contribute to the understanding of the molecular mechanisms involved in the infection process and may reveal novel avenues to minimize consequences of poplar rust and other rust diseases.

The last decade of genomic and post-transcriptomic research on the *M. larici-populina*–poplar–larch pathosystem contributed to clarification of several molecular stages during the

infection process (Lorrain et al. 2018; Persoons et al. 2022). Petre et al. (2020) showed that *M. larici-populina* expresses both host-specific and generalist CSEPs in its secretome during the infection process of its two host plants. dos Santos et al. (2021) showed that during in planta expression, unrelated CSEPs from *M. larici-populina* can act on overlapping plant functions such as MAPK signaling pathways. Several *M. larici-populina* CSEPs have been reported to promote host susceptibility in the oomycete pathosystem *Hyalonoperonospora arabidopsidis–Arabidopsis thaliana* (Germain et al. 2018). Mlp124478 binds a TGA1a promoter motif to suppress the expression of genes involved in plant immune response (Ahmed et al. 2018), whereas Mlp37347 promotes virulence through specific interactions with glutamate decarboxylase 1 (GAD1) and causes cellular changes, such as enhancing plasmodesmatal flux and inhibiting callose deposition (Rahman et al. 2021). The functional characterization of more and more CSEPs revealed various targeted cellular compartments (Germain et al. 2018; Lorrain et al. 2019; Petre et al. 2016). In general, the CSEP translocation mechanism remains unclear. Notable exceptions are Chloroplast-targeted protein 1 (CTP1) and CTP2 from *M. larici-populina* and CTP3 from *Melampsora lini*, which use a host transit peptide mimicry to reach the chloroplast in *Nicotiana benthamiana* leaf epidermis (Petre et al. 2016). Interestingly, an increasing number of candidate effectors show a putative chloroplast localization, such as AvrMlp7, Mlp124111, and Mlp72983 (Germain et al. 2018; Lorrain et al. 2018; Louet et al. 2023). In addition, stromules were observed in a previous study of CTP1, CTP2, and CTP3 (Petre et al. 2016). These results expand our understanding of the molecular mechanisms involved in *M. larici-populina* infection process and highlight the importance of chloroplast targeting.

Beyond photosynthetic activity and cellular homeostasis, chloroplasts are also involved in plant immunity. Under abiotic or biotic stresses, chloroplasts in *N. benthamiana* have been observed to cluster around the nucleus, and several studies suggested that chloroplast-derived reactive oxygen species act as signal molecules for programmed cell death induction related to the hypersensitive response (HR) (Caplan et al. 2015; Lukan et al. 2020; Su et al. 2018). Chloroplast morphology can also rapidly adapt, particularly by inducing stroma-filled tubule projections called "stromules" (Brunkard et al. 2015; Caplan et al. 2015; Schattat and Klösgen 2011). Stromules are potentially involved in transmitting signals from the chloroplast to other subcellular locations, but the molecular mechanisms remain to be defined (Brunkard et al. 2015; Caplan et al. 2015; Schattat et al. 2012a, b). Stromule induction seems to be shared by plastids in response to a wide variety of abiotic and biotic stresses (Erickson et al. 2018; Holzinger et al. 2008; Lukan et al. 2023). For example, recognition of the bacterial effector XANTHOMONAS OUTER PROTEIN Q (XopQ) in *N. benthamiana* by the nucleotide-binding leucine-rich repeat resistance (NLR) protein receptor RECOGNITION OF XOPQ1 (ROQ1) induces stromules and programmed cell death through ENHANCED DISEASE SUSCEPTIBILITY 1 (EDS1) and the NLR helpers N-REQUIRED GENE 1 (NRG1) and ACTIVATED DISEASE RESISTANCE GENE 1 (ADR1) cascade (Prautsch et al. 2023; Schultink et al. 2017). Unfortunately, the current lack of diversity of stromule elicitors, including from different pathosystems, is one of the limitations to their further characterization (Schultink et al. 2017).

As a strict heteroecious species, *M. larici-populina* provided a unique opportunity to assess protein pairs that are very similar in terms of amino acid composition but each expressed on a specific host species. In the present study, we first selected 9 candidate effectors out of 1,184 candidates based on host-specificity transcriptomics and sequence homology. We determined that despite a high level of sequence homology, their subcellular localizations could differ. Yeast two-hybrid protein–protein interaction screening against both host proteomes demonstrated that some effectors pairs interacted with conserved targets from the two hosts. Finally, we observed that some effectors induced stromule formation. Therefore, we quantified the stromules induced by these CSEPs and characterized the first stromule inducers from a fungal pathogen. Moreover, these quantifications led to the unveiling of a new stromule-induction cascade as well as new tools to study stromule-related regulation cascades.

Results

Transcriptomic and homology analyses reveal host-specific and homologous candidate effectors

Figure 1 displays the selection process criteria to retain host-specific and homologous effectors. This process was applied for all candidate secreted effector families reported by Hacquard et al. (2012) (family 7 is depicted here as an example). In Figure 1A, urediniospore (USP) and basidiospore (BSD) (which are considered noninfective spore stages) transcripts show levels of expression lower than in infected poplar leaves (Poplar) as well as in pycnia and aecia during larch biotrophic infection stages (Larch). This indicates that CSEPs from family 7 are specific to the infection process. Mlp52166 is annotated as poplar specific based on its 16.2 times higher expression during poplar infection than during larch infection. In a similar way, Mlp72983 is 62.3 times more expressed in larch than in poplar, defining a larch-specific annotation. Single effectors as well as families with fewer than three members were not considered. Only 60 CSEPs, segregating in eight families, met our criteria. Figure 1B demonstrates the second step of the selection process, namely alignments and similarity scoring based on the CSEP mature sequences, which identified the most similar pairs (threshold set at a minimum of 50% homology). Pairs were then selected if they had a different host specificity. Figure 1C quantitatively summarizes our selection process. Table 1 lists the three candidate effector pairs from families 1, 33, and 51, as well as one triplet from family 7, of CSEPs selected for further analysis. Family 7 was chosen as a triplet based on high similarity scores between both Mlp52166-Mlp72983 (76.9%) and Mlp52166-Mlp86274 (58.7%) pairs.

Protein–protein interaction screening reveals specific and homologous interactors

Because members of the selected effector pairs most likely emerged through divergent evolution, it is tempting to speculate that their sequence divergences emerged to adapt to their target(s) in the hosts in which they are expressed. This presented the opportunity to investigate whether their targets in the different hosts were indeed homologous. Larch and poplar libraries were each built from six RNA replicates isolated from healthy, fully extended poplar leaves and larch needles. As illustrated in steps 1 and 2 of Figure 2A, each effector was screened against the library corresponding to its assigned host specificity (Mlp104486, Mlp51690, Mlp107359, and Mlp52166 against the poplar library; Mlp123281, Mlp53845, Mlp108708, Mlp72983, and Mlp86274 against the larch library). Then, a second screen revealed candidate interactors also able to interact with the homologous effector of the investigated pair (steps 3 and 4 of Figure 2A). Despite four screening attempts, Mlp51690, Mlp107359, and Mlp108708 did not yield any interacting partner (unique candidate interactors are also available in Supplementary Table S3). As shown in Figure 2B, family 1 (Mlp104486 and Mlp123281) and family 7 (Mlp52166, Mlp72983, and Mlp86274) identified 10 and 3 pair/triplet-specific common candidate interactors, respectively, supporting that these effectors could have similar function(s) in both hosts.

Host-specific and homologous CSEPs localize in several cell compartments

Subcellular localization of CSEPs has significantly contributed to effector functional characterization (Lorrain et al. 2018). Here we sought to assess whether CSEPs that display similar sequences fused with reporter fluorescent proteins localized to the same cellular organelles in the heterologous system *N. benthamiana*. Figure 3A depicts the localization of the enhanced green fluorescent protein (eGFP) as a control. Mlp104486 colocalizes with a small interfering RNA (siRNA) body marker (Fig. 3B). In addition to nuclear accumulation, Mlp123281,

Mlp51690, Mlp107359, Mlp72983, and Mlp86274 colocalize with chlorophyll autofluorescence, despite belonging to four different families (Fig. 3C, D, F, I, and J). Moreover, Mlp123281, Mlp51690, and Mlp72983 share a similar colocalization with the chloroplastic nucleoid marker SWIB6::RFP (Fig. 3C, D, and I, right panel). As shown in Figure 3G and in Supplementary Figure S1, Mlp108708 colocalizes with five different cellular markers along the secretory pathway: endoplasmic reticulum (ER), Golgi, late endosome and multivesicular bodies (LE/MVBs), tonoplast and plasma membrane (Fig. 3G; Supplementary Fig. S2). Mlp53845 and Mlp52166 (Fig. 3E and

Fig. 1. Screening process of host-specific and homologous candidate secreted effector proteins (CSEPs). **A,** Inter-family screening step aiming at the host-specificity annotation of candidate effectors and identification of families with more than two members that have different host specificity. Heat map of family 7 is shown as an example of a family with different host specificity. USP, urediniospores; BSD, basidiospores. **B,** Intra-family screening step selecting pairs of candidate effectors with the highest homology score. Phylogenetic tree of family 7 is shown as an example for the selection of homologs. **C,** Population of candidate effector proteins screened though the process.
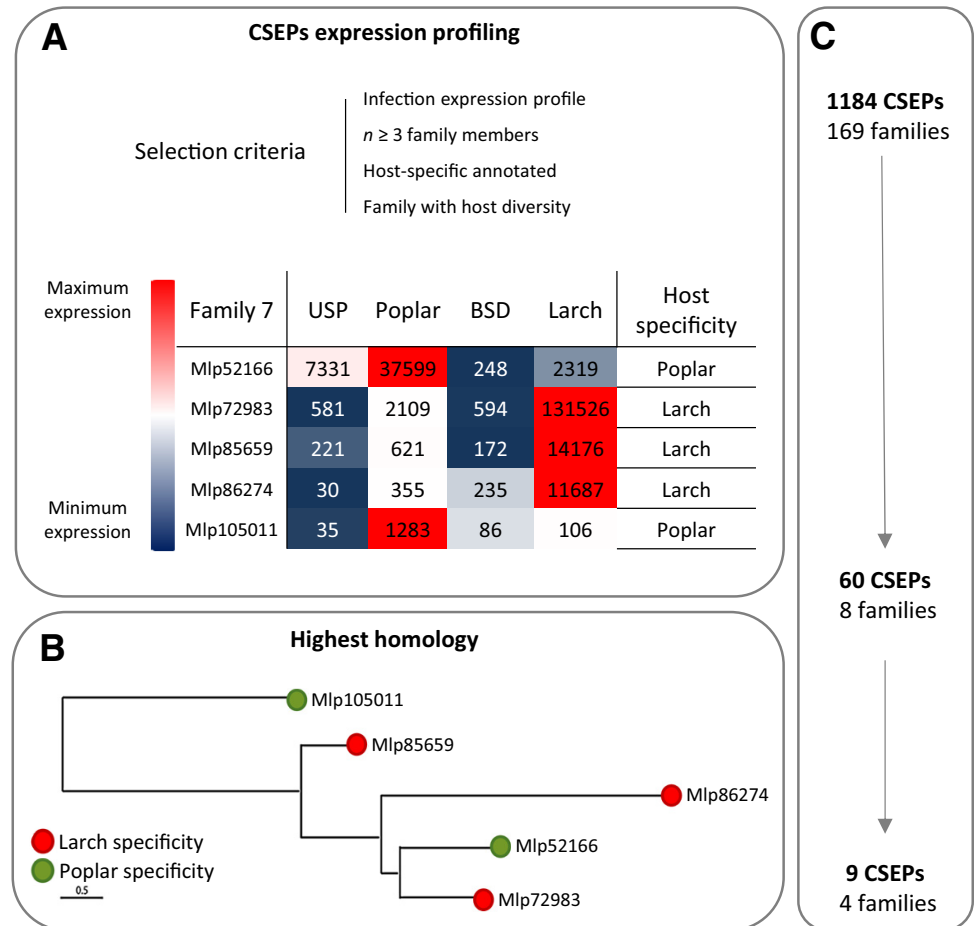
Table 1. Characteristics of host-specific and homologous candidate secreted effector proteins (CSEPs) of *Melampsora larici-populina*

Family[a]	Protein ID[b]	CPG/class[c]	Similarity (%)[d]	Host specificity[e]	Length[f]	Cysteine (%)[g]
1 (111)	Mlp104486	Class 1	86.5	Poplar	105 (24)	9.5
	Mlp123281	Class 1		Larch	105 (25)	9.5
33 (6)	Mlp51690	CPG462	85.4	Poplar	146 (26)	6.8
	Mlp53845	CPG462		Larch	147 (26)	6.8
51 (4)	Mlp107359	CPG1075	86.2	Poplar	117 (20)	0
	Mlp108708	CPG1075		Larch	144 (20)	0
7 (12)	Mlp52166	CPG332-333	76.9[φ]	Poplar	196 (24)	4.6
	Mlp72983	CPG332-333	55.9[ʊ]	Larch	195 (26)	4.1
	Mlp86274	CPG332-333	58.7[º]	Larch	223 (22)	4

[a] Family number annotated by Duplessis et al. (2011) and Hacquard et al. (2012). The number of family members is indicated in parentheses.

[b] ID based on the *M. larici-populina* genome 98AG31 version 2.0, available on the Joint Genome Institute MycoCosm web portal (https://mycocosm.jgi.doe.gov/Mellp2_3/Mellp2_3.home.html).

[c] CPG, cluster of paralogous genes according to Hacquard et al. (2012).

[d] Amino acid similarity between family members calculated by EMBOSS matcher explorer https://www.bioinformatics.nl/cgi-bin/emboss/matcher: [φ]similarity between Mlp52166 and Mlp72983; [º]similarity between Mlp52166 and Mlp86274; [ʊ]similarity between Mlp86274 and Mlp72983.

[e] Host specificity determined by this study selection criteria.

[f] Length of mature protein in amino acids. Length of the putative signal peptide is in parentheses (identified by SignalP version 4.1).

[g] Cysteine richness of CSEP mature length.

H) displayed a similar localization to the eGFP control; such a localization was therefore deemed inconclusive. These results illustrate that homologous CSEPs can target different cell compartments, while CSEPs with no sequence similarity and belonging to different families can target the same organelles.

Host-specific and homologous CSEPs induce stromules dependently and independently of EDS1

Through our subcellular localization observations, we noticed that some CSEPs seemed to induce an unusual number of stromules. To assess whether this was significant, we quantified stromules using XopQ as a positive control. None of the *M. larici-populina* CSEPs induced an HR after 10 days postinoculation (dpi) in *N. benthamiana*, whereas stromule-inducing XopQ induced the expected HR (Fig. 4A). Family 1 CSEPs did not induce stromules in wild-type *N. benthamiana* plants, while members

of families 7, 33, and 51 significantly induced stromule formation (Fig. 4B). As EDS1 is required for XopQ stromule induction, we used *eds1* knockout *N. benthamiana* plants to assess its role in the formation of the CSEP-induced stromules (Fig. 5). In this context, CSEP still did not induce HR at 10 dpi and, as expected, XopQ no longer induced HR because of the interrupted effector triggered immunity (ETI) signal pathway in the *eds1* mutant (Prautsch et al. 2023) (Fig. 5A). Interestingly, the *eds1* mutation inhibited stromule induction by family 33 members (Mlp51690 and Mlp53845) (Fig. 5B). Also, *eds1* plants showed a significant decrease of induction for Mlp107359 and Mlp108708 of family 51 and Mlp52166 of family 7, although not to the basal level. Surprisingly, there were no significant changes for Mlp72983 and Mlp86274, the two other members of family 7. Finally, we investigated the requirement for NRG1 downstream in the known stromule induction cascade regard-

Fig. 2. *Melampsora larici-populina* candidate effectors from families 1 and 7 share family-specific candidate interactors. **A,** Four types of screening were performed for each family. Step 1: Poplar-specific candidate effectors were screened against poplar library. Step 2: Larch-specific effectors were screened against larch library. Step 3: The candidate effectors specific to larch were tested for their interaction with poplar candidate interactors obtained from step 1. Step 4: The candidate effectors specific to poplar were tested for their interaction with larch candidate interactors obtained from step 2. **B,** Blue square lists common candidate interactors shared by Mlp104486 and Mlp123281 from family 1. Orange square groups common candidate interactors shared by Mlp52166, Mlp72983, and Mlp86274 from family 7. Purple square shows common candidate interactors shared by Mlp52166 and Mlp86274 from family 7. Sequence similarity rate is detailed in between the two circles. GAL4, transcriptional activation domain from yeast; BD, binding domain; AD, activator domain.
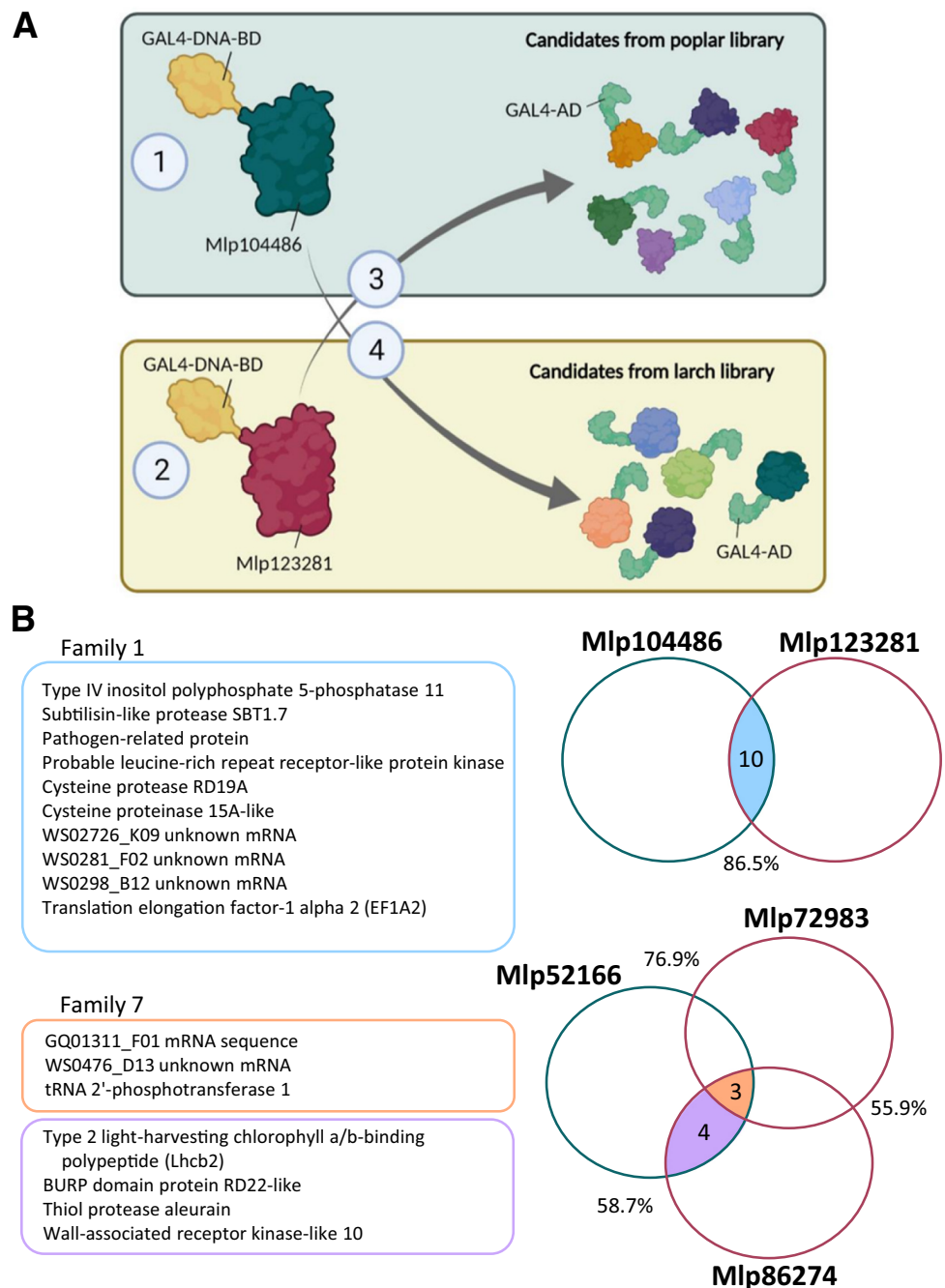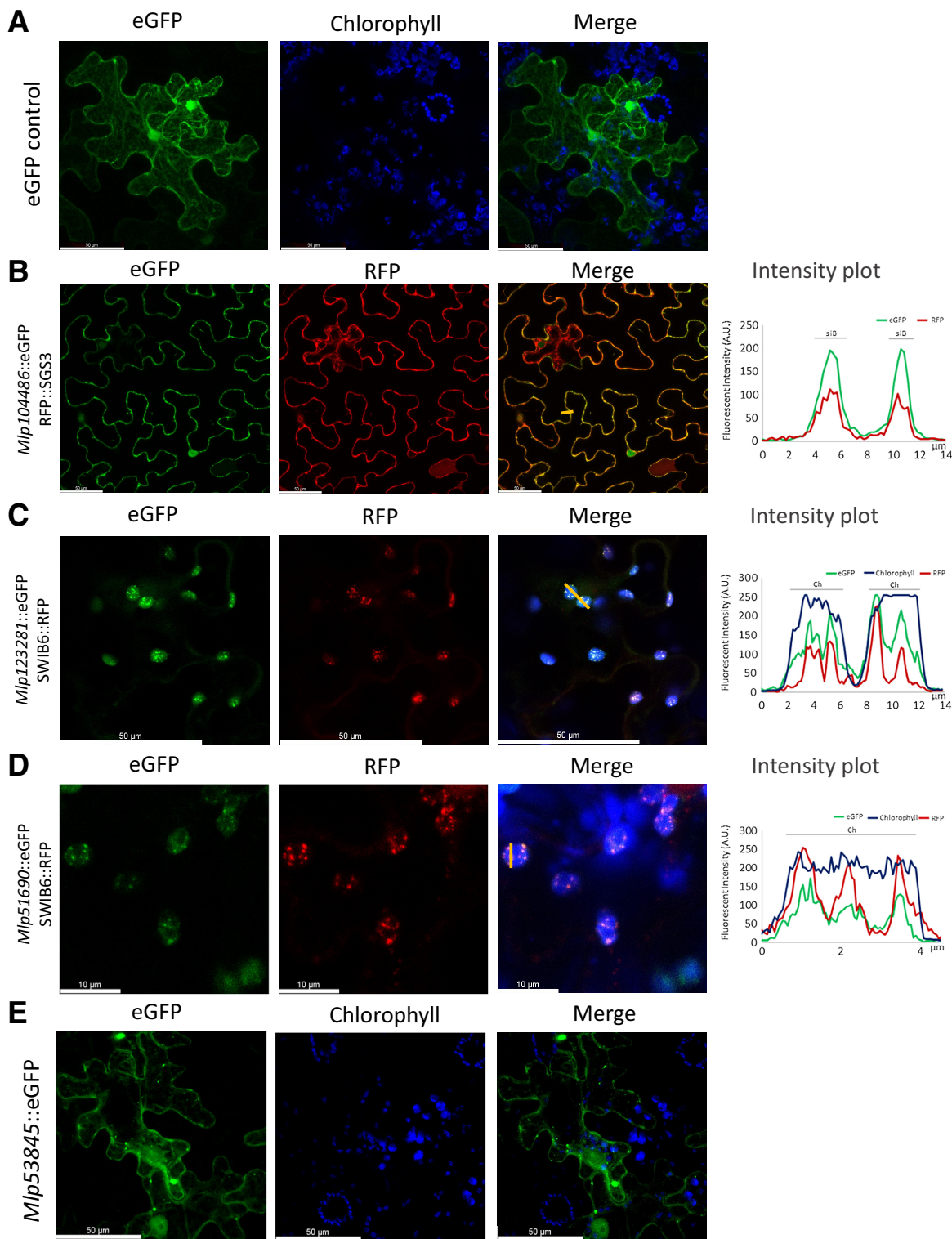
Fig. 3. Candidate effectors target various cell compartments. Confocal microscopy images show the fluorescence of *Agrobacterium tumefaciens*-infiltrated abaxial epidermis of *Nicotiana benthamiana* between 1 and 3 days postinoculation (dpi) depending on maximum signal. CSEP::eGFP, green panels; chloroplastic autofluorescence, blue panels; potential subcellular markers, red panels. Intensity plots illustrate colocalization results supported by the authors. **A,** *z*-Stack accumulation of free enhanced green fluorescent protein (eGFP). **B,** Focal plane of Mlp104486::eGFP coexpressed with siRNA body marker RFP::SGS3 (*n* = 14). **C,** Focal plane of Mlp123281::eGFP coexpressed with chloroplastic nucleoid marker SWIB6::RFP (*n* = 12). **D,** Focal plane of Mlp51690::eGFP coexpressed with chloroplastic nucleoid marker SWIB6::RFP (*n* = 9). **E,** *z*-Stack accumulation of Mlp53845::eGFP showing localization to the nucleus, cytosol, and cytosolic bodies (unconclusive) (*n* = 8). **F,** *z*-Stack accumulation of Mlp107359::eGFP showing chloroplastic and cytosolic localization (*n* = 9). **G,** Focal plane of Mlp108708::eGFP coexpressed with vacuole marker mCherry::RAB7 (*n* = 22). **H,** *z*-Stack accumulation of Mlp52166::eGFP showing nucleus and cytosol localization (unspecific) (*n* = 5). **I,** Focal plane of Mlp72983::eGFP coexpressed with chloroplastic nucleoid marker SWIB6::RFP (*n* = 16). **J,** Focal plane of Mlp86274::eGFP, which colocalizes with chloroplastic autofluorescence (*n* = 11). Arrowhead shows a stromule. Number of independent plant replicates transiently expressing CSEP::eGFP with or without cellular markers. Orange bars show origin of intensity plot. CSEP, candidate secreted effector protein; RFP, red fluorescent protein; siB, siRNA bodies; Ch, chloroplast; V, vacuole. Subcellular markers from Nelson et al. (2007), Melonek et al. (2012), and Ivanov and Harrison (2014).

(Continued)

ing the requirement for NRG1 (Fig. 6). Figure 6A and Supplementary Figure S2A show that XopQ does not caused an HR in the two independent plant lines NbFNR::eGFP_*nrg1-4* and NbFNR::eGFP_*nrg1-5*, similar to Mlp72983 and Mlp86274, which also did not. Mlp72983- and Mlp86274-triggered stromule induction was significantly reduced but not completely abolished (Fig. 6B; Supplementary Fig. S2B). From these results (Figs. 4, 5, and 6; Supplementary Fig. S2), we conclude that these host-specific and homologous candidate secreted effectors do not induce HR and shared stromule induction patterns among families: family 1 did not induce any stromules, family 33 induction is *esd1* dependent, family 51 and Mlp52166 from

Fig. 3. (*Continued from previous page*)
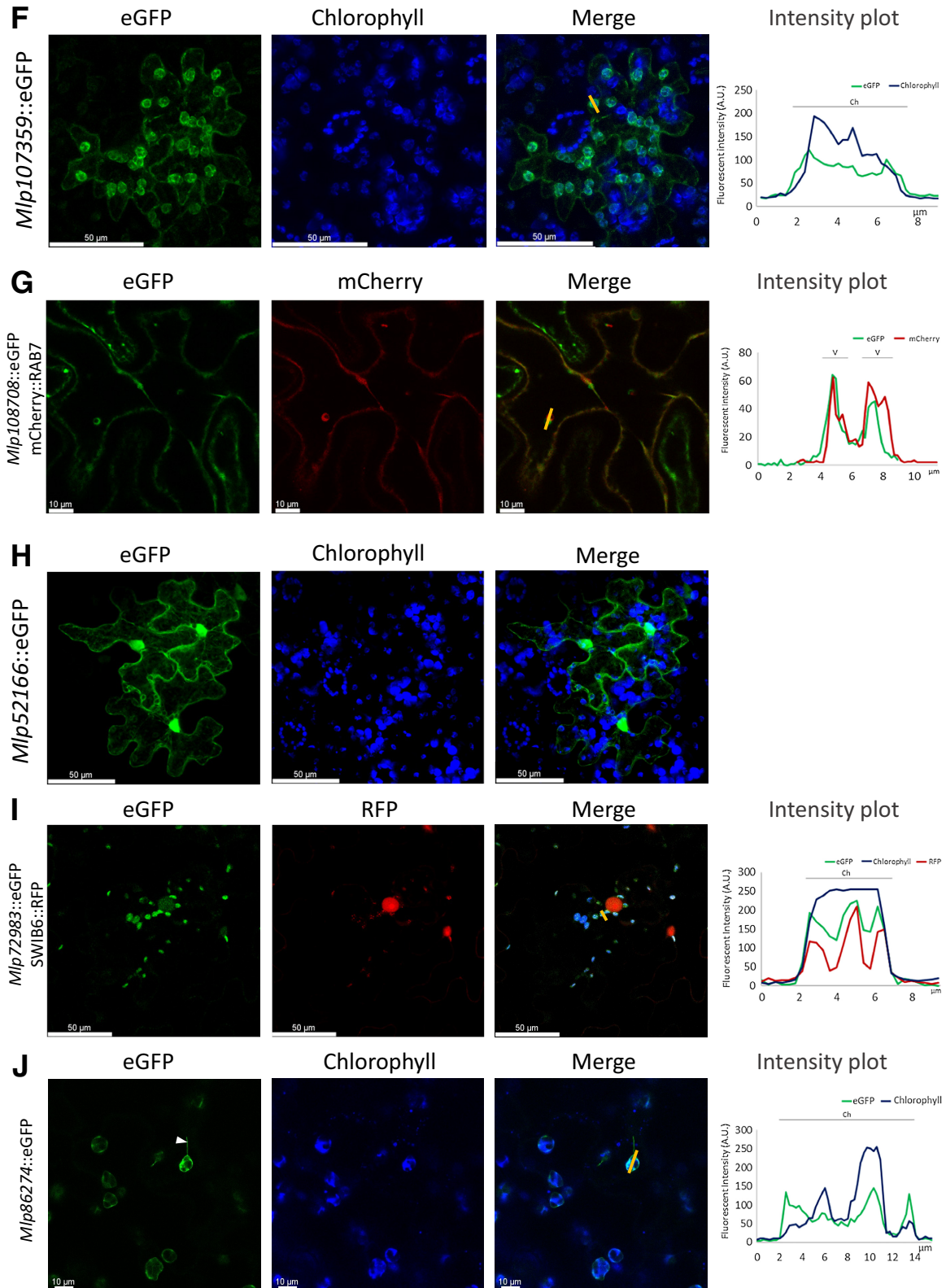
family 7 induced stromules in a partially *eds1*-dependent manner, and finally Mlp72983 and Mlp86274 from family 7 induced stromules in an *eds1*-independent but partially *nrg1*-dependent way.

Discussion

In this study, we identified and characterized homologous CSEPs that show different host-specificity expression profiles. The rationale for this selection was that if two effectors have very close sequence homology in a given CSEP family but preferential expression in one of the two hosts, then they could potentially interact with similar proteins in each of both hosts and interfere with similar biological processes. One pair and the triplet of CSEPs shared common protein interactors between family members. Interestingly, five out of the nine CSEPs showed a partial or exclusive chloroplastic subcellular localization in *N. benthamiana*. Two of the pairs and the triplet induced stromules in three different ways in *N. benthamiana*: EDS1 dependent, partially EDS1 dependent, and EDS1 independent but partially NRG1 dependent. These results add to the growing evidence that chloroplasts play a key role in the immune response (Caplan et al. 2015; Kretschmer et al. 2020; Kumar et al. 2018; Littlejohn et al. 2021; Serrano et al. 2016).

The main hypothesis driving the present study was that homolog CSEPs may accomplish the same major functions to as-sist the infection process in a host-specific way. The two selected members from family 1, Mlp104486 and Mlp123281, have 86.5% sequence similarity. They also share 10 common candidate host interactors and partially share their subcellular localization, and both did not induce stromule formation. Similarly, the two selected members of family 51, Mlp107359 and Mlp108708, have high sequence similarity (86.2%); however, neither interacted with host proteins screened by yeast two-hybrid assays. Both triggered EDS1-dependent stromule formation, but they have different cellular localizations: Mlp107359 is chloroplastic, whereas Mlp108708 colocalizes with cellular markers along the secretory pathway (ER, trans-Golgi network, LE, vacuole, and plasma membrane). The two selected members of family 3, Mlp51690 and Mlp53845, have 85.4% sequence similarity and both induced EDS1-dependent stromules. They, however, do not share candidate host protein interactors or subcellular localization. Mlp51690 is localized in chloroplast nucleoids, whereas Mlp53845's localization is inconclusive, as it is similar to the eGFP alone (i.e., nuclear and cytosolic). Finally, two of the selected members of family 7, Mlp72983 and Mlp86274, only share 55.9% sequence similarity, but despite this relatively low similarity, both translocated to the chloroplastic compartment, shared common candidate host protein interactors, and induced partially *nrg1*-dependent stromules.

These results confirmed that homology based on sequence similarity, as first established by Xiang (2006), may not be a suffi-

Fig. 4. *Melampsora larici-populina* candidate secreted effector proteins (CSEPs) from families 33, 51, and 7 induce stromules in *Nicotiana benthamiana*. **A,** Response of NbFNR::eGFP plants at 10 days postinoculation (dpi). **B,** Ratio of stromules per chloroplast at 72 h postinfiltration (hpi) ($n = 36$, 3 replicates on 12 plants). Asterisk shows $P \leq 0.05$ significantly different based on Mann-Whitney test. Red bar indicates significant differences between AIM (*Agrobacterium* infiltration medium) and mOrange negative controls versus CSEPs. Blue bar indicates significant differences between XopQ:mOrange positive control versus CSEPs. eGFP, enhanced green fluorescent protein.
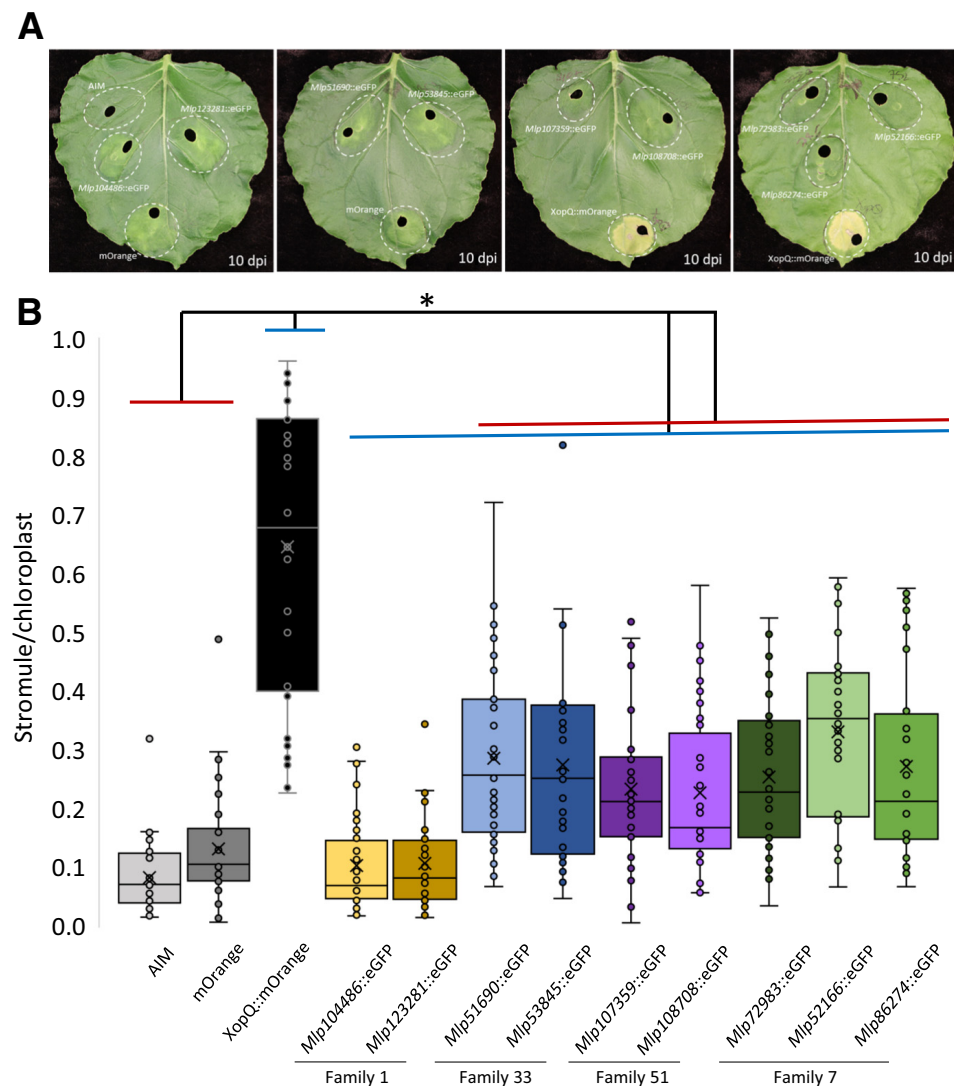
cient characteristic to predict protein characteristics (dos Santos et al. 2021; Xiang 2006). Actual protein function prediction software combines several parameters such as deep learning, protein structure, protein sequence, or protein–protein interaction data to reach better accuracy (Dawson et al. 2017; Waterhouse et al. 2018; Zhang et al. 2017; Zheng et al. 2022). Indeed, it has been demonstrated that unrelated CSEPs displaying different subcellular localization can trigger similar genes or metabolic deregulation patterns (dos Santos et al. 2021; Germain et al. 2018). However, these transcriptomic and metabolomic analyses did not include the homologous CSEP pairs that were characterized in the present study and were done in the heterologous plant *A. thaliana*. Therefore, it appears that although sequence homology is a good tool to group sequences within a family, it should not be used to infer that two CSEPs will have the same target or localization. Nevertheless, while the mechanisms of protein sorting in cells are relatively conserved, it is possible that the larch effectors did not reach their true subcellular localization caused by the evolutionary gap between *Nicotiana* (angiosperm) and larch (gymnosperm). In this study, sequence homology appears to be a good proxy to evaluate which cellular processes are perturbed by effectors, as effectors that share high sequence homology did not share the same localization but had similar impact on stromule induction.

Identification of CSEP interactors is an important aspect to consider in their functional characterization. The poor annotation of the larch proteome was a major hindrance for our study, and we performed reverse screenings to circumvent this obstacle. As illustrated in Figure 2A, we studied protein–protein interactions of poplar-specific CSEPs against larch candidate interactors and of larch-specific CSEPs against poplar candidate interactors. Moreover, our low rate of protein interactor identification mirrors previous findings of Petre et al. (2015), who identified specific interactors for only 5 out of the 20 *M. larici-populina* CSEPs transiently expressed in *N. benthamiana* and screened by co-immunoprecipitation followed by liquid chromatography-tandem mass spectrometry (Petre et al. 2015). In the interaction screen, CSEPs of both families 1 and 7 displayed positive interaction with several proteins that remain to be annotated, and 7 out of 10 common candidate interactors of family 1 were annotated. Interestingly, Mlp104486 and Mlp123281 interacted with RESPONSE TO DEHYDRATATION 19 A (RD19A) and a 15A-like cysteine protease, two PAPAIN-LIKE CYSTEINE PROTEASE (PLCPs). Several PLCPs are reported to trigger the immune response and programmed cell death (Dervisi et al. 2022; Dong et al. 2014; Misas Villamil et al. 2019). Moreover, RD19 interacts with the bacterial effector PSEUDOMONAS OUTER PROTEIN P2 (PopP2) and translocates to

Fig. 5. The *eds1* deletion suppresses, reduces, or does not change stromule induction of candidate effectors from families 33, 51, and 7. **A,** Response of NbFNR::eGFP_*eds1* plants at 10 days postinoculation (dpi). **B,** Ratio of stromules per chloroplast at 72 h postinfiltration (hpi) of NbFNR::eGFP_*eds1* plants compared with wild type (*n* = 24, 3 replicates on 8 plants). Asterisks show *P* ≤ 0.05 significantly different based on Mann-Whitney test. Red bar indicates significant differences between AIM (*Agrobacterium* infiltration medium) and mOrange negative controls versus candidate secreted effector proteins (CSEPs). Blue bar indicates significant differences between XopQ::mOrange positive control versus CSEPs. eGFP, enhanced green fluorescent protein.
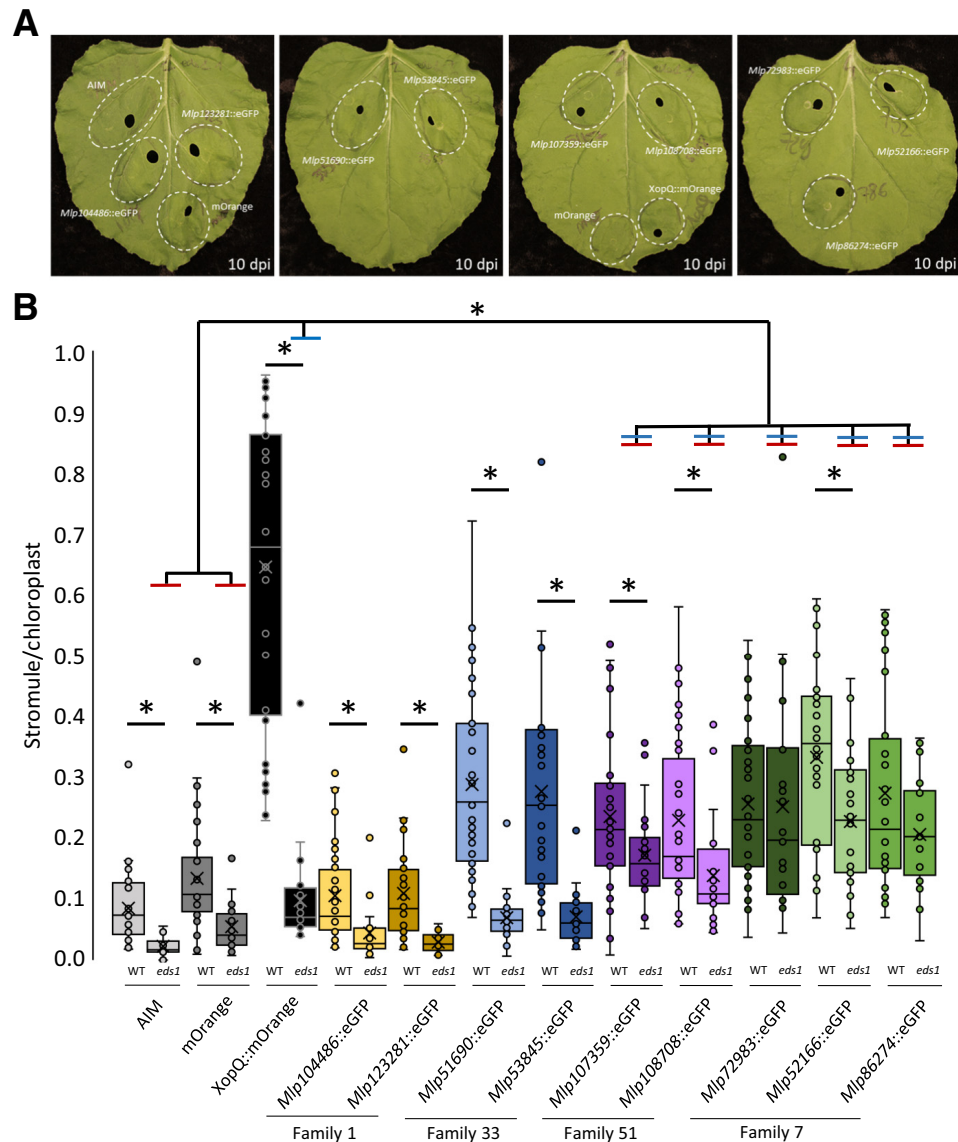
the nucleus (Bernoux et al. 2008). Localization of Mlp104486 and Mlp123281 to the nucleus, cytosol, and cytosolic bodies is consistent with such an interaction. Putative DNA-binding sites, predicted by DRNApred (Yan and Kurgan 2017), were identified in Mlp104486 and Mlp123281 sequences. These effectors interacted with TRANSLATION ELONGATION FACTOR 1 ALPHA 2 (EF1A2), which contributes to the translation initiation and elongation steps (Hwang et al. 2015). Moreover, Mlp104486 also interacted with three different types of RNA polymerase subunits, one ribosomal subunit, and the transcription factor GATA TF5, which is reported to mediate abiotic stress responses in poplar (An et al. 2020). The potential function of *M. larici-populina* CSEPs interfering with the plant transcription machinery has already been reported (Ahmed et al. 2018; dos Santos et al. 2021). Our results here suggest that CSEPs of family 1 might possibly also act as transcription modulators.

The triplet of CSEPs from family 7 shares three common candidate interactors: two unannotated proteins and the TRNA

2′-PHOSPHOTRANSFERASE 1 (TRPT1) enzyme, which concludes the last step of tRNA processing and is involved in pleiotropic effects on plant growth and immunity when disrupted (Soprano et al. 2018). The multiple TRTP1 subcellular localizations in nucleus, cytosol, mitochondria, and chloroplast partially fit with family 7 CSEP localization (Englert et al. 2007). Recently, the *Puccinia striiformis* f. sp. *tritici* effector Pst_A23 was characterized to suppress plant defense by directly binding a pre-mRNA splice site (Tang et al. 2022). Mlp72983 is one of the best-characterized *M. larici-populina* CSEPs. It was already observed as partially chloroplastic in *A. thaliana* stable lines, whereas transient expression in *N. benthamiana* revealed chloroplastic nucleoid localization. However, several replicates also showed nuclear speckle accumulation. Moreover, Mlp72983 is predicted to have a nuclear localization signal and a DNA-binding site. Triplet partners Mlp52166 and Mlp86274 do not share those predicted domains. Mlp72983 also downregulates important plant defense-related genes such as WRKY33, PR1, PDF1.2a, PDF1.2b, PDF1.2c, and RESPI-

Fig. 6. Mlp72983 and Mlp86274 induce NRG1-dependent stromules. **A,** Response of NbFNR::eGFP_*nrg1-4* plants at 10 days postinoculation (dpi). **B,** Ratio of stromules per chloroplast at 72 h postinfiltration (hpi) of NbFNR::eGFP_*nrg1-4* plants compared with wild type (*n* = 18, 3 replicates on 6 plants). Asterisks show *P* ≤ 0.05 significantly different based on Mann-Whitney test. AIM, *Agrobacterium* infiltration medium. Blue bar indicates significant differences between XopQ::mOrange positive control versus candidate secreted effector proteins (CSEPs). eGFP, enhanced green fluorescent protein.
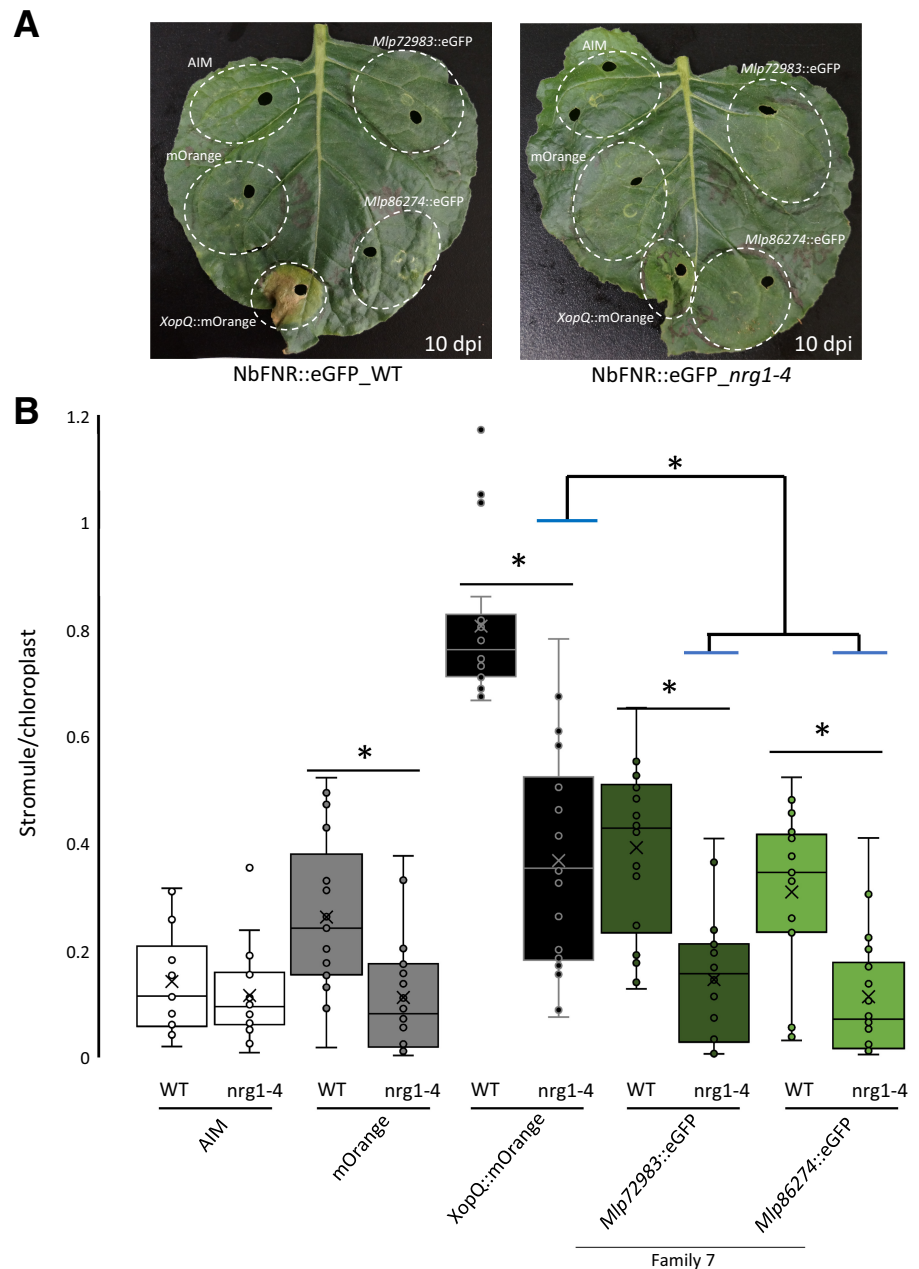
RATORY BURST OXIDASE HOMOLOGS (RBOHD) in *A. thaliana* and enhances the growth of the oomycete *Hyaloperonospora arabidopsidis* Noco2 when expressed in planta (dos Santos et al. 2021; Germain et al. 2018). *Arabidopsis halleri* PDF1 is reported to have an antifungal activity against *Fusarium oxysporum* f. sp. *melonis* (Shahzad et al. 2013). Mlp72983 may thus directly or indirectly modulate host transcription.

Despite the lack of protein interactor identification for some of the selected CSEPs, it is staggering that a majority localized to chloroplast and/or induced stromules. Chloroplasts are more and more considered to be a stress sensor for cell homeostasis and are closely related to immune response and HR triggers (Caplan et al. 2015; Erickson et al. 2018; Kumar et al. 2018; Prautsch et al. 2023). Petre et al. (2016) highlighted that the *M. larici-populina* candidate effector protein CTP1 induced an increasing number of stromules without precisely quantifying them. Hence, our study is the first to characterize stromule-inducing fungal candidate secreted effectors proteins. With the knowledge that that viral and bacterial effector proteins can trigger stromule formation, our study and the Petre et al. (2016) study support that stromules act as a general stress-related chloroplastic reaction in biotic stress conditions (Hanson and Hines 2018). Moreover, Mlp72983 and Mlp86274 revealed new stromule induction pathways: EDS1-independent but partially NRG1-dependent. The first proposed molecular cascade of stromule induction has been published (Prautsch et al. 2023). The stromule induction signaling cascade based on XopQ induction is shown in Figure 7A. In Figure 7B, we added our results to the same cascade. The present results may enlarge the general role of stromules in a pathosystem. It should be pointed out that XopQ elicits stromule induction through its recognition by the NLR ROQ1, which in turn triggers ETI. The effectors investigated in this study originate from *M. larici-populina*, which is not a pathogen that infects *Nicotiana*, and thus it would be very unlikely that an NLR–effector recognition occurs; thus, for the *M. larici-populina* effector, stromule induction is not occurring in the context of ETI. The stromule induction without HR raises the question of whether the stromule may also benefit the pathogen in a specific context. Because one role of effectors is to attenuate the immune response, and stromules are induced during ROQ1-triggered immunity, a more intuitive result would have been a decrease in stromule production. Therefore, the seven new inducers represent new tools to study the mechanisms related to stromule induction.

More efforts will be needed to further characterize stromule induction and the precise role of stromules during infection in the *M. larici-populina* larch–poplar pathosystems. Because *M. larici-populina* is a rust fungus, most of its infection cycle occurs in chloroplast-rich mesophyll cells; therefore the manipulation of the chloroplast could be a cell type-dependent coevolution, which could explain why such a large proportion of the effector studied herein targets the chloroplast (5/9) or induces stromule formation (7/9). A possible way to further investigate stromule induction could be to set up a screening based on CSEP–host protein structure prediction and docking, but sparse host proteomes, particularly the larch proteome, still limit such approaches. Our results present additional limitations to take into consideration when assessing candidate effector function and putative targets and provide novel tools to dissect the mechanisms related to stromule induction.

Materials and Methods

Plasmids

Candidate secreted effector sequences (genome JGI Mellp version 2.0) were synthesized by Gene Universal and amplified without signal peptide following the Gateway protocol (Persoons et al. 2022; Supplementary Table S1). Amplicons were cloned in a pDONR221 entry vector and then in a pK7FWG2 destination vector (Karimi et al. 2002). Cellular

Fig. 7. New biological tools to explore stromule induction pathway(s). **A,** The bacterial effector XopQ pathway contributes to building the first pathway of stromule induction (Prautsch et al. 2023). **B,** Seven out of nine *Melampsora larici-populina* candidate effectors characterized in this study showed singular patterns to induce stromules in *Nicotiana benthamiana*. ETI and PCD are shown lighter compared with case A because they are not induced in *Nicotiana benthamiana* with the studied candidate secreted effector proteins. They represent seven possible avenues to understanding molecular mechanisms involved in biotic stromule induction. ETI, effector triggered immunity; PCD, programmed cell death.
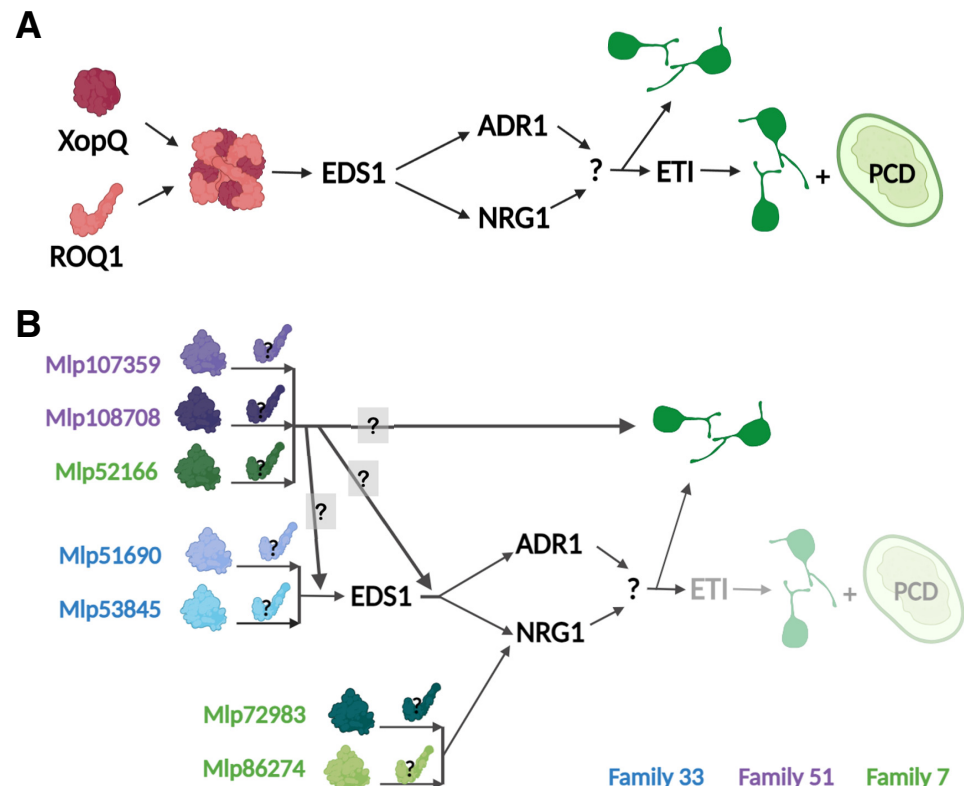
markers mCherry::HDEL (ER), mCherry::SYP41 (trans-Golgi network), mCherry::RAB5 (LE/MVBs), mCherry::RAB7 (vacuole), and PIP2a::mCherry are from Ivanov and Harrison (2014). Stromule controls, XopQ::mOrange and mOrange, are from Erickson et al. (2018).

Bacterial material and growth conditions

Cloning, and DNA propagation were performed in electro-competent *Escherichia coli* DH10B or DH5α strains cultivated on Luria-Bertani (LB) medium with appropriate antibiotics. *Agrobacterium tumefaciens* strain GV3101 (pMP90) was transformed and selected on yeast extract peptone medium containing rifampicin (100 µg/ml), gentamycin (25 µg/ml), and spectinomycin (50 µg/ml) or kanamycin (50 µg/ml). Yeast strains Y187 and Y2HGold were grown on yeast extract peptone dextrose medium with appropriate selective amino acid deficiency and/or aureobasidin A (200 ng/ml). Transformed *E. coli* TOP10 strain were selected on LB medium with ampicillin (50 µg/ml) to rescue and propagate candidate plasmids from the first step of the yeast two-hybrid assay.

Plant material and growth conditions

N. benthamiana plants were grown in growth chambers (BioChambers) or greenhouses at 22°C with 16-h day/8-h night, and 60% humidity. Stromule quantification needed wild-type and knocked-out *N. benthamiana* lines with plastid labeled by constitutive expression of the transit peptide of FERREDOXIN NADP(H) OXIDOREDUCTASE (FNR) fused to eGFP (Schattat and Klösgen 2011). The *eds1-1* plants are homozygous knockouts (Ordon et al. 2017). Independent knocked-out *nrg1-4* and *nrg1-5* lines were used (Ordon et al. 2021).

Transcriptome and sequence analysis

M. larici-populina pathotype 98AG31 transcriptomes were collected from Duplessis et al. (2011) and Lorrain et al. (2018) (see Guerillot et al. 2021). Transcripts from urediniospores and basidiospores were considered noninfectious stages. Infection transcriptomes were respectively extracted from infected poplar leaves (haustoria-producing stage; poplar specificity) as well as pycnia and aecia from infected larch needles (larch specificity). To ensure effector homology, screening focused on pairs of effectors classified in the same CSEP families according to Hacquard et al. (2012). Selected pairs shared the following criteria: presence of a signal peptide, sequence of fewer than 300 amino acids, more than 50% of sequence similarity, expressed in both host during infectious stage transcriptomes, and having a minimum of 10-fold ratio in one host versus the other (Guerillot et al. 2021).

cDNA library

Around 100 mg of healthy needles and leaves were used for RNA extraction following the lithium chloride method (Chang et al. 1993). Briefly, tissues were crushed in liquid nitrogen with a mortar and pestle. Then, 750 µl of extraction buffer (2% cetyltrimethylammonium bromide, 2% polyvinyl pyrrolidone, 100 mM Tris-HCl pH 8, 25 mM ethylenediamine tetraacetic acid pH 8, 2 M NaCl, 0.5 g/liter spermidine, and 2% β-mercaptoethanol freshly added) were added and incubated 10 min at 65°C. On ice, 500 µl of chloroform:isoamyl alcohol (24:1) were added and centrifuged 7 min at 13,000 rpm and 4°C. The aqueous phase was transferred and added to an equivalent volume of LiCl (10 M) for 3 h at –20°C. After centrifugation (20 min, 13,000 rpm, 4°C), the pellet was washed with 400 µl of cold 80% ethanol, centrifuged, dried, and resuspended with 40 µl of RNase-free water. All samples showed a minimum of 8.5/10 RNA Quality Indicator (RQI) estimated by Experion

(Automated Electrophoresis System, Bio-Rad). Six replicates were pooled for yeast two-hybrid library preparation.

Candidate secreted effector interactor screening

Protein–protein interaction screening was made by yeast two-hybrid assay technologies provided by Clontech Takara Bio. Poplar and larch libraries were built by Make Your Own "Mate & Plate" Library System for Yeast Two-Hybrid Screening. Then, 4 µg of cDNA was cotransformed with 3 µg of linearized pGADT7-Rec in Y187 competent cell according to the Yeastmaker Yeast Transformation System 2 protocol (Clontech Inc.). The poplar library and larch library were harvested and stored at –80°C at 2.23×10^7 UFC/ml and 1.66×10^7 UFC/ml, respectively. Mature candidate effector sequences were cloned in pGBKT7 plasmid by digestion-ligation (*Eco*RI-*Sal*I). According to the same yeast transformation protocol, each candidate secreted effector was transformed in Y2HGold strain. Screening by yeast mating followed the Matchmaker Gold Yeast Two-Hybrid System (Clontech Inc.) protocol and quality-control requirement (2% of mating generating a minimum of 1×10^6 diploids). Candidate targets were amplified by colony-PCR (Supplementary Table S2) and sequenced (Nanuq, Génome Québec). Candidate interactors were annotated based on the best hit on BLAST (tBlastn, v. 2.8.0-α). Hits were considered false positives if they were: found in negative controls, found in independent previous lab work, hits with more than two nonhomologous candidate secreted effectors, or annotated in a different subcellular localization than the effector (Rajagopala and Uetz 2011). The putative localization of each prey was determined with the Protein Databank (https://www.rcsb.org) and TAIR (https://www.arabidopsis.org). For reverse screening, each plasmid was extracted by miniprep (FroggaBio) and tested against the candidate effector of the alternate host.

Transient protein expression in *N. benthamiana*

A. tumefaciens GV3101 (pMP90) containing specific plasmids for cellular markers or candidate effector was grown overnight and centrifuged for 5 min at 5,000 rpm. The pellet was resuspended in $MgCl_2$ 10 mM and 150 µM acetosyringone to reach 0.5 OD_{600nm} for cellular localization or 0.2 OD_{600nm} for stromule quantification. Candidate secreted effector and cellular marker were mixed in a 1:1 ratio for the colocalization study (Ivanov and Harrison 2014). After 1 h of room temperature incubation, *Agrobacterium* solution was abaxially agroinfiltrated in the youngest fully expanded leaves of 4- to 6-week old *N. benthamiana* plants with a needleless syringe. Based on maximal signal expression, samples were observed either at 48 h or 72 h postinfiltration. These localizations were observed a minimum of five times in independent replicates.

Image acquisition and processing

Leaf tissues were vacuum-infiltrated with sterile water before observation on glass slides. Subcellular localization and *nrg1* stromule counting were performed on a Leica TCS SP8 (Leica Microsystems) with oil objectives HC PL APO CS2 40× or 63×. eGFP, RFP/mCherry/mOrange, and far red were excited and collected at 488/500 to 525 nm, 552/600 to 625 nm, and 638/650 to 700 nm, respectively. Lasers were set at 4% intensity. Images were acquired and processed with LAS AF Lite software (Leica Microsystems). Wild-type and *eds1* stromule quantifications were performed on the epifluorescence microscope AxioObserver Z1 (Zeiss) equipped with an X-Cite fluorescence light source and an MRm monochrome camera using a 40×/0.75 NA EC PLAN NEOFLUAR lens. eGFP and mOrange fluorescence were recorded with 38 HE and 43 HE filter cubes, respectively (Carl Zeiss), and acquired and processed with Zen-

Blue software. Images and *z*-stacks were performed on abaxial epidermis.

The stromule quantification protocol started by combining each image from a *z*-stack acquisition (maximum of 20 optical sections through 10-μm depth along the *z*-axis) into a single image, as previously described in Schattat and Klösgen (2009). Stromule quantification was assisted by MT-BCellCounter, hosted on ImageJ, Java (Franke et al. 2015) and counted in a semi-automated fashion (Savage et al. 2021).

Literature Cited

Ahmed, M. B., Santos, K. C. G. d., Sanchez, I. B., Petre, B., Lorrain, C., Plourde, M. B., Duplessis, S., Desgagné-Penix, I., and Germain, H. 2018. A rust fungal effector binds plant DNA and modulates transcription. Sci. Rep. 8:14718.

An, Y., Zhou, Y., Han, X., Shen, C., Wang, S., Liu, C., Yin, W., and Xia, X. 2020. The GATA transcription factor GNC plays an important role in photosynthesis and growth in poplar. J. Exp. Bot. 71:1969-1984.

Bernoux, M., Timmers, T., Jauneau, A., Brière, C., de Wit, P. J. G. M., Marco, Y., and Deslandes, L. 2008. RD19, an *Arabidopsis* cysteine protease required for RRS1-R–mediated resistance, is relocalized to the nucleus by the *Ralstonia solanacearum* PopP2 effector. Plant Cell 20:2252-2264.

Brasier, C. M. 2008. The biosecurity threat to the UK and global environment from international trade in plants. Plant Pathol. 57:792-808.

Brunkard, J. O., Runkel, A. M., and Zambryski, P. C. 2015. Chloroplasts extend stromules independently and in response to internal redox signals. Proc. Natl. Acad. Sci. U.S.A. 112:10044-10049.

Caplan, J. L., Kumar, A. S., Park, E., Padmanabhan, M. S., Hoban, K., Modla, S., Czymmek, K., and Dinesh-Kumar, S. P. 2015. Chloroplast stromules function during innate immunity. Dev. Cell 34:45-57.

Chaloner, T. M., Gurr, S. J., and Bebber, D. P. 2021. Plant pathogen infection risk tracks global crop yields under climate change. Nat. Clim. Change 11:710-715.

Chang, S. J., Puryear, J., and Cairney, J. 1993. A simple and efficient method for isolating RNA from pine trees. Plant Mol. Biol. Rep. 11:113-116.

Dawson, N. L., Lewis, T. E., Das, S., Lees, J. G., Lee, D., Ashford, P., Orengo, C. A., and Sillitoe, I. 2017. CATH: An expanded resource to predict protein function through structure and sequence. Nucleic Acids Res. 45:D289-D295.

Dervisi, I., Haralampidis, K., and Roussis, A. 2022. Investigation of the interaction of a papain-like cysteine protease (RD19c) with selenium-binding protein 1 (SBP1) in *Arabidopsis thaliana*. Plant Sci. 315:111157.

Dong, S., Stam, R., Cano, L. M., Song, J., Sklenar, J., Yoshida, K., Bozkurt, T. O., Oliva, R., Liu, Z., Tian, M., Win, J., Banfield, M. J., Jones, A. M. E., van der hoorn, R. A. L., and Kamoun, S. 2014. Effector specialization in a lineage of the Irish potato famine pathogen. Science 343:552-555.

dos Santos, K. C. G., Pelletier, G., Séguin, A., Guillemette, F., Hawkes, J., Desgagné-Penix, I., and Germain, H. 2021. Unrelated fungal rust candidate effectors act on overlapping plant functions. Microorganisms 9:996.

Duplessis, S., Cuomo, C. A., Lin, Y.-C., Aerts, A., Tisserant, E., Veneault-Fourrey, C., Joly, D. L., Hacquard, S., Amselem, J., Cantarel, B. L., Chiu, R., Coutinho, P. M., Feau, N., Field, M., Frey, P., Gelhaye, E., Goldberg, J., Grabherr, M. G., Kodira, C. D., Kohler, A., Kües, U., Lindquist, E. A., Lucas, S. M., Mago, R., Mauceli, E., Morin, E., Murat, C., Pangilinan, J. L., Park, R., Pearson, M., Quesneville, H., Rouhier, N., Sakthikumar, S., Salamov, A. A., Schmutz, J., Selles, B., Shapiro, H., Tanguay, P., Tuskan, G. A., Henrissat, B., Van de Peer, Y., Rouzé, P., Ellis, J. G., Dodds, P. N., Schein, J. E., Zhong, S., Hamelin, R. C., Grigoriev, I. V., Szabo, L. J., Martin, F. 2011. Obligate biotrophy features unraveled by the genomic analysis of rust fungi. Proc. Natl. Acad. Sci. U.S.A. 108:9166-9171.

Duplessis, S., Lorrain, C., Petre, B., Figueroa, M., Dodds, P. N., and Aime, M. C. 2021. Host adaptation and virulence in heteroecious rust fungi. Annu. Rev. Phytopathol. 59:403-422.

Englert, M., Latz, A., Becker, D., Gimple, O., Beier, H., and Akama, K. 2007. Plant pre-tRNA splicing enzymes are targeted to multiple cellular compartments. Biochimie 89:1351-1365.

Erickson, J. L., Adlung, N., Lampe, C., Bonas, U., and Schattat, M. H. 2018. The *Xanthomonas* effector XopL uncovers the role of microtubules

in stromule extension and dynamics in *Nicotiana benthamiana*. Plant J. 93:856-870.

Franke, L., Storbeck, B., Erickson, J. L., Rödel, D., Schröter, D., Möller, B., and Schattat, M. S. 2015. The 'MTB Cell Counter' a versatile tool for the semi-automated quantification of sub-cellular phenotypes in fluorescence microscopy images. A case study on plastids, nuclei and peroxisomes. J. Endocytobiosis Cell Res. 26:31-42.

Germain, H., Joly, D. L., Mireault, C., Plourde, M. B., Letanneur, C., Stewart, D., Morency, M.-J., Petre, B., Duplessis, S., and Séguin, A. 2018. Infection assays in *Arabidopsis* reveal candidate effectors from the poplar rust fungus that promote susceptibility to bacteria and oomycete pathogens. Mol. Plant Pathol. 19:191-200.

Guerillot, P., Morin, E., Kohler, A., Louet, C., and Duplessis, S. 2021. A comprehensive collection of transcriptome data to support life cycle analysis of the poplar rust fungus *Melampsora larici-populina*. bioRxiv 453710.

Hacquard, S., Delaruelle, C., Legué, V., Tisserant, E., Kohler, A., Frey, P., Martin, F., and Duplessis, S. 2010. Laser capture microdissection of uredinia formed by *Melampsora larici-populina* revealed a transcriptional switch between biotrophy and sporulation. Mol. Plant-Microbe Interact. 23:1275-1286.

Hacquard, S., Joly, D. L., Lin, Y.-C., Tisserant, E., Feau, N., Delaruelle, C., Legué, V., Kohler, A., Tanguay, P., Petre, B., Frey, P., Van der Peer, Y., Rouzé, P., Martin, F., Hamelin, R. C., and Duplessis, S. 2012. A comprehensive analysis of genes encoding small secreted proteins identifies candidate effectors in *Melampsora larici-populina* (poplar leaf rust). Mol. Plant-Microbe Interact. 25:279-293.

Hacquard, S., Petre, B., Frey, P., Hecker, A., Rouhier, N., and Duplessis, S. 2011. The poplar-poplar rust interaction: Insights from genomics and transcriptomics. J. Pathog. 2011:716041.

Hanson, M. R., and Hines, K. M. 2018. Stromules: Probing formation and function. Plant Physiol. 176:128-137.

Holzinger, A., Kwok, E. Y., and Hanson, M. R. 2008. Effects of *arc3*, *arc5* and *arc6* mutations on plastid morphology and stromule formation in green and nongreen tissues of *Arabidopsis thaliana*. Photochem. Photobiol. 84:1324-1335.

Hwang, J., Lee, S., Lee, J.-H., Kang, W.-H., Kang, J.-H., Kang, M.-Y., Oh, C.-S., and Kang, B.-C. 2015. Plant translation elongation factor 1Bβ facilitates *Potato virus X* (PVX) infection and interacts with PVX triple gene block protein 1. PLoS One 10:e0128014.

Ivanov, S., and Harrison, M. J. 2014. A set of fluorescent protein-based markers expressed from constitutive and arbuscular mycorrhiza-inducible promoters to label organelles, membranes and cytoskeletal elements in *Medicago truncatula*. Plant J. 80:1151-1163.

Karimi, M., Inzé, D., and Depicker, A. 2002. GATEWAY™ vectors for *Agrobacterium*-mediated plant transformation. Trends Plant Sci. 7:193-195.

Kretschmer, M., Damoo, D., Djamei, A., and Kronstad, J. 2020. Chloroplasts and plant immunity: Where are the fungal effectors? Pathogens 9:19.

Kumar, A. S., Park, E., Nedo, A., Alqarni, A., Ren, L., Hoban, K., Modla, S., McDonald, J. H., Kambhamettu, C., Dinesh-Kumar, S. P., and Caplan, J. L. 2018. Stromule extension along microtubules coordinated with actin-mediated anchoring guides perinuclear chloroplast movement during innate immunity. eLife 7:e23625.

Kuzmin, D. A., Feranchuk, S. I., Sharov, V. V., Cybin, A. N., Makolov, S. V., Putintseva, Y. A., Oreshkova, N. V., and Krutovsky, K. V. 2019. Stepwise large genome assembly approach: A case of Siberian larch (*Larix sibirica* Ledeb). BMC Bioinf. 20:37.

Littlejohn, G. R., Breen, S., Smirnoff, N., and Grant, M. 2021. Chloroplast immunity illuminated. New Phytol. 229:3088-3107.

Lorrain, C., Gonçalves dos Santos, K. C., Germain, H., Hecker, A., and Duplessis, S. 2019. Advances in understanding obligate biotrophy in rust fungi. New Phytol. 222:1190-1206.

Lorrain, C., Petre, B., and Duplessis, S. 2018. Show me the way: Rust effector targets in heterologous plant systems. Curr. Opin. Microbiol. 46:19-25.

Louet, C., Saubin, M., Andrieux, A., Persoons, A., Gorse, M., Pétrowski, J., Fabre, B., De Mita, S., Duplessis, S., Frey, P., and Halkett, F. 2023. A point mutation and large deletion at the candidate avirulence locus *AvrMlp7* in the poplar rust fungus correlate with poplar RMlp7 resistance breakdown. Mol. Ecol. 32:2472-2483.

Lukan, T., Pompe-Novak, M., Baebler, Š., Tušek-Žnidarič, M., Kladnik, A., Križnik, M., Blejec, A., Zagorščak, M., Stare, K., Dušak, B., Coll, B., Pollman, S., Morgiewicz, K., Hennig, J., and Gruden, K. 2020. Precision transcriptomics of viral foci reveals the spatial regulation of immune-signaling genes and identifies *RBOHD* as an important player in the incompatible interaction between potato virus Y and potato. Plant J. 104:645-661.

Lukan, T., Županič, A., Mahkovec Povalej, T., Brunkard, J. O., Kmetič, M., Juteršek, M., Baebler, Š., and Gruden, K. 2023. Chloroplast redox state

changes mark cell-to-cell signaling in the hypersensitive response. New Phytol. 237:548-562.

Melonek, J., Matros, A., Trösch, M., Mock, H.-P., and Krupinska, K. 2012. The core of chloroplast nucleoids contains architectural SWIB domain proteins. Plant Cell 24:3060-3073.

Misas Villamil, J.C., Mueller, A. N., Demir, F., Meyer, U., Ökmen, B., Schulze Hüynck, J., Breuer, M., Dauben, H., Win, J., Huesgen, P. F., and Doehlemann, G. 2019. A fungal substrate mimicking molecule suppresses plant immunity via an inter-kingdom conserved motif. Nat. Commun. 10:1576.

Nelson, B. K., Cai, X., and Nebenführ, A. 2007. A multicolored set of in vivo organelle markers for co-localization studies in Arabidopsis and other plants. Plant J. 51:1126-1136.

Ordon, J., Gantner, J., Kemna, J., Schwalgun, L., Reschke, M., Streubel, J., Boch, J., and Stuttmann, J. 2017. Generation of chromosomal deletions in dicotyledonous plants employing a user-friendly genome editing toolkit. Plant J. 89:155-168.

Ordon, J., Martin, P., Erickson, J. L., Ferik, F., Balcke, G., Bonas, U., and Stuttmann, J. 2021. Disentangling cause and consequence: Genetic dissection of the *DANGEROUS MIX2* risk locus, and activation of the DM2h NLR in autoimmunity. Plant J. 106:1008-1023.

Persoons, A., Hayden, K. J., Fabre, B., Frey, P., De Mita, S., Tellier, A., and Halkett, F. 2017. The escalatory Red Queen: Population extinction and replacement following arms race dynamics in poplar rust. Mol. Ecol. 26:1902-1918.

Persoons, A., Maupetit, A., Louet, C., Andrieux, A., Lipzen, A., Barry, K. W., Na, H., Adam, C., Grigoriev, I. V., Segura, V., Duplessis, S., Frey, P., Halkett, F., and De Mita, S. 2022. Genomic signatures of a major adaptive event in the pathogenic fungus *Melampsora larici-populina*. Genome Biol. Evol. 14:evab279.

Petre, B., and Duplessis, S. 2022. A decade after the first Pucciniales genomes: A bibliometric snapshot of (post) genomics studies in three model rust fungi. Front. Microbiol. 13:989580.

Petre, B., Lorrain, C., Saunders, D. G. O., Win, J., Sklenar, J., Duplessis, S., and Kamoun, S. 2016. Rust fungal effectors mimic host transit peptides to translocate into chloroplasts. Cell. Microbiol. 18:453-465.

Petre, B., Lorrain, C., Stukenbrock, E. H., and Duplessis, S. 2020. Host-specialized transcriptome of plant-associated organisms. Curr. Opin. Plant Biol. 56:81-88.

Petre, B., Saunders, D. G. O., Sklenar, J., Lorrain, C., Win, J., Duplessis, S., and Kamoun, S. 2015. Candidate effector proteins of the rust pathogen *Melampsora larici-populina* target diverse plant cell compartments. Mol. Plant-Microbe Interact. 28:689-700.

Pinon, J., and Frey, P. 2005. Interactions between poplar clones and *Melampsora* populations and their implications for breeding for durable resistance. Pages 139-154 in: Rust Diseases of Willow and Poplar. CABI Publishing, Wallingford, U.K.

Prautsch, J., Erickson, J. L., Özyürek, S., Gormanns, R., Franke, L., Lu, Y., Marx, J., Niemeyer, F., Parker, J. E., Stuttmann, J., and Schattat, M. H. 2023. Effector XopQ-induced stromule formation in *Nicotiana benthamiana* depends on ETI signaling components ADR1 and NRG1. Plant Physiol. 191:161-176.

Rahman, M. S., Madina, M. H., Plourde, M. B., dos Santos, K. C. G., Huang, X., Zhang, Y., Laliberté, J.-F., and Germain, H. 2021. The fungal effector Mlp37347 alters plasmodesmata fluxes and enhances susceptibility to pathogen. Microorganisms 9:1232.

Rajagopala, S. V., and Uetz, P. 2011. Analysis of protein–protein interactions using high-throughput yeast two-hybrid screens. Pages 1-29 in: Network Biology: Methods and Applications. G. Cagney and A. Emili, eds. Springer, New York, NY.

Savage, Z., Duggan, C., Toufexi, A., Pandey, P., Liang, Y., Segretin, M. E., Yuen, L. H., Gaboriau, D. C. A., Leary, A. Y., Tumtas, Y., Khandare, V., Ward, A. D., Botchway, S. W., Bateman, B. C., Pan, I., Schattat, M.,

Sparkes, I., and Bozkurt, T. O. 2021. Chloroplasts alter their morphology and accumulate at the pathogen interface during infection by *Phytophthora infestans*. Plant J. 107:1771-1787.

Schattat, M. H., Griffiths, S., Mathur, N., Barton, K., Wozny, M. R., Dunn, N., Greenwood, J. S., and Mathur, J. 2012a. Differential coloring reveals that plastids do not form networks for exchanging macromolecules. Plant Cell 24:1465-1477.

Schattat, M. H., and Klösgen, R. B. 2009. Improvement of plant cell microscope images by use of 'Depth of Field' - extending software. Endocytobiosis Cell Res. 19:11-19.

Schattat, M. H., and Klösgen, R. B. 2011. Induction of stromule formation by extracellular sucrose and glucose in epidermal leaf tissue of *Arabidopsis thaliana*. BMC Plant Biol. 11:115.

Schattat, M. H., Klösgen, R. B., and Mathur, J. 2012b. New insights on stromules: Stroma filled tubules extended by independent plastids. Plant Signal. Behav. 7:1132-1137.

Schultink, A., Qi, T., Lee, A., Steinbrenner, A. D., and Staskawicz, B. 2017. Roq1 mediates recognition of the Xanthomonas and Pseudomonas effector proteins XopQ and HopQ1. Plant J. 92:787-795.

Serrano, I., Audran, C., and Rivas, S. 2016. Chloroplasts at work during plant innate immunity. J. Exp. Bot. 67:3845-3854.

Shahzad, Z., Ranwez, V., Fizames, C., Marquès, L., Le Martret, B., Alassimone, J., Godé, C., Lacombe, E., Castillo, T., Saumitou-Laprade, P., Berthomieu, P., and Gosti, F. 2013. *Plant Defensin type 1 (PDF 1)*: Protein promiscuity and expression variation within the *Arabidopsis* genus shed light on zinc tolerance acquisition in *Arabidopsis halleri*. New Phytol. 200:820-833.

Soprano, A. S., Smetana, J. H. C., and Benedetti, C. E. 2018. Regulation of tRNA biogenesis in plants and its link to plant growth and response to pathogens. Biochim. Biophys. Acta Gene Regul. Mech. 1861:344-353.

Su, J., Yang, L., Zhu, Q., Wu, H., He, Y., Liu, Y., Xu, J., Jiang, D., and Zhang, S. 2018. Active photosynthetic inhibition mediated by MPK3/MPK6 is critical to effector-triggered immunity. PLoS Biol. 16:e2004122.

Sun, C., Xie, Y.-H., Li, Z., Liu, Y.-J., Sun, X.-M., Li, J.-J., Quan, W.-P., Zeng, Q.-Y., Van de Peer, Y., and Zhang, S.-G. 2022. The *Larix kaempferi* genome reveals new insights into wood properties. J. Integr. Plant Biol. 64:1364-1373.

Tang, C., Xu, Q., Zhao, J., Yue, M., Wang, J., Wang, X., Kang, Z., and Wang, X. 2022. A rust fungus effector directly binds plant pre-mRNA splice site to reprogram alternative splicing and suppress host immunity. Plant Biotechnol. J. 20:1167-1181.

Tuskan, G. A., Difazio, S., Jansson, S., Bohlmann, J., Grigoriev, I., Hellsten, U., Putnam, N., Ralph, S., Rombauts, S., Salamov, A., et al. 2006. The genome of black cottonwood, *Populus trichocarpa* (Torr. & Gray). Science 313:1596-1604.

van Esse, H. P., Reuber, T. L., and van der Does, D. 2020. Genetic modification to improve disease resistance in crops. New Phytol. 225:70-86.

Waterhouse, A., Bertoni, M., Bienert, S., Studer, G., Tauriello, G., Gumienny, R., Heer, F. T., de Beer, T. A. P., Rempfer, C., Bordoli, L., Lepore, R., and Schwede, T. 2018. SWISS-MODEL: Homology modelling of protein structures and complexes. Nucleic Acids Res. 46:W296-W303.

Xiang, Z. 2006. Advances in homology protein structure modeling. Curr. Protein Pept. Sci. 7:217-227.

Yan, J., and Kurgan, L. 2017. DRNApred, fast sequence-based method that accurately predicts and discriminates DNA-and RNA-binding residues. Nucleic Acids Res. 45:e84.

Zhang, C., Freddolino, P. L., and Zhang, Y. 2017. COFACTOR: Improved protein function prediction by combining structure, sequence and protein–protein interaction information. Nucleic Acids Res. 45:W291-W299.

Zheng, W., Wuyun, Q., Zhou, X., Li, Y., Freddolino, P. L., and Zhang, Y. 2022. LOMETS3: Integrating deep learning and profile alignment for advanced protein template recognition and function annotation. Nucleic Acids Res. 50:W454-W464.